J. Membrane Biol. 86, 1–7 (1985)

The Journal of
Membrane Biology


*Topical Review*

# Biological Membrane Structure as "Seen" by X-ray and Neutron Diffraction Techniques

J.K. Blasie, L. Herbette*, and J. Pachence**
Departments of Chemistry and Biochemistry/Biophysics, University of Pennsylvania, Philadelphia, Pennsylvania 19104, and Department of Biology, Brookhaven National Laboratory, Upton, New York 11973

## Introduction

The structure of biological membranes is generally liquid-crystalline in nature. The molecular components usually exhibit thermally-driven internal motions characteristic of polyatomic molecules, translational motions in the plane of the membrane, and rotational motions about axes perpendicular to the plane of the membrane. The molecular components usually exhibit only very limited (in extent) translational motions perpendicular to the membrane plane or rotational motions about axes in the membrane plane. This dynamic structural organization of the membrane is analogous to that found within a single lamella of multilamellar liquid-crystals, i.e., so-called "smectics" [26]. In special cases, some of the molecular components of the membrane may be segregated into domains possessing various degrees of long-range crystalline order in two dimensions over the membrane plane.

Of the various physical techniques currently utilized for probing the structure of biological membranes (including all forms of optical spectroscopy and microscopy, X-ray spectroscopy, electron paramagnetic resonance, nuclear magnetic resonance, electron spectroscopy and microscopy, etc.), only techniques involving the elastic scattering/diffraction of short wavelength radiation ($\lambda \sim 1$A), specifically X-ray and neutron diffraction, are capable of providing detailed structural information over a wide range of length scales from 1–$10^4$A concerning the time average of the dynamic membrane structure. As a result, these two techniques can, in principle, provide key information concerning both the intramolecular structure of membrane components and the intermolecular ordering of these molecular components within the overall dynamic structural organization of the biological membrane.

X-rays are scattered elastically by atomic electrons [22]. When the energy of the incident X-ray photon is such that it cannot induce any excitations of the atomic electrons, potential scattering of the incident X-ray occurs with the scattering amplitude for the atom being proportional to the atomic number. When the energy of the incident X-ray photon is tuned to that capable of inducing an excitation of the atomic electrons, resonance scattering of the incident X-ray occurs, significantly modifying the scattering amplitude of the atom as compared with the potential scattering case. Hence, the X-ray scattering amplitude of a particular atomic site in a molecule can be altered either by changing the atom itself (often difficult to achieve isomorphously) or by tuning the incident X-ray photon energy to that capable of inducing electronic excitations of the atom (currently technically limited to atoms heavier than $Z \sim 20$). Neutrons are scattered elastically by atomic nuclei [2]. When the energy of the incident neutron is *not* comparable to that of a quasi-discrete energy level of the "compound nucleus" (composed of the incident neutron and the scattering nucleus), potential scattering of the incident neutron occurs; the potential scattering of thermal neutrons from most atomic nuclei is very similar in amplitude. When the energy of the incident neutron is comparable to that of a quasi-discrete energy level of the compound nucleus, resonance scattering of the incident neutron occurs; the resonance scattering of thermal neutrons from particular atomic nuclei differs dramatically from the more usual poten-

**Key Words** X-ray diffraction · neutron diffraction · resonance scattering · membrane protein · lipid bilayer · time-averaged · time-resolved · elastic scattering

* *Current address:* Department of Medicine, University of Connecticut, Health Center, Farmington, CT 06032.

** *Current address:* Helitrex Corp., P.O. 2041, Princeton, New Jersey 08540.

tial scattering from other nuclei. Hence, the neutron scattering amplitude of a particular atomic site in a molecule can, in some cases, be altered by changing the isotope of the atom at that site. The most notable among a few such isotopic pairs of atoms which can be readily interchanged isomorphously at a particular molecular site possessing a large difference in the elastic scattering of thermal neutrons is that of hydrogen (resonance) *versus* deuterium (potential).

The elastic scattering for short-wavelength radiation from a collection of molecules composing a single membrane in the form of a planar sheet occurs primarily along two principal directions denoted[1] as $Q_\perp$ perpendicular to the membrane plane and $Q_\parallel$ parallel to the membrane plane [13, 26]. The elastic scattering along $Q_\perp$ arises from the time-averaged scattering-density profile $\rho(z)$ for the membrane. The scattering-density profile $\rho(z)$ is the projection of all atomic scattering centers along vectors lying in the various membrane planes perpendicular to the $z$-axis onto the $z$-axis [13]. The elastic scattering along $Q_\parallel$ arises from the time-averaged scattering density in the membrane plane $\rho(x,y)$ where $\rho(x,y)$ is the projection of all atomic scattering centers along vectors perpendicular to the membrane plane onto the $x$-$y$ plane [13].

The elastic scattering from a planar single membrane sheet may be enhanced by a factor ranging from $N$ to $N^2$ by stacking an ensemble of $N$ such sheets into an oriented multilayer in which all the planar sheets are co-parallel [13]. The enhancement factor depends upon the nature of long-range order in the stacking of the sheets along the stacking direction $z$. The elastic scattering along $Q_\perp$ from the oriented multilayer is that for a planar single-membrane sheet modulated by interference effects arising from the classical interference of X-ray photons or neutrons scattered from different membrane sheets in the oriented multilayer [13]. It should be noted that the clear distinction between such elastic scattering along $Q_\perp$ and $Q_\parallel$ may be lost due to their superposition in the elastic scattering from an ensemble of randomly oriented single-membrane sheets or membrane multilayers [26].

Generally, the elastic scattering along $Q_\parallel$ (and $Q_\perp$) is invariant to rotation of the planar single-membrane sheet or the oriented multilayer about the $z$-axis because of the liquid-crystalline nature of the membrane structure and the lack of rotational order about the $z$-axis from sheet to sheet in an oriented multilayer [13, 26]. Only in the instances of very large two-dimensionally crystalline domains (e.g. $> 10$ $\mu$m diameter) in single-membrane sheets and in oriented multilayers possessing a significant degree of rotational order about the $z$-axis from sheet to sheet for $N$ small ($N < 5$) is this not the case for elastic scattering along $Q_\parallel$. As a result, in the more general case, the elastic scattering data along $Q_\parallel$ is usually analyzed via a radial Patterson function $P(r)$ which requires *only* the observable *scattering amplitude data* as a function of $Q_\parallel$ (i.e., scattering-angle $2\theta$) [10, 15, 21, 23]. The resolution (or highest spatial frequency component) in the radial Patterson function derived via an appropriate Fourier-Bessel transformation of the $Q_\parallel$ scattering data depends on the largest value of $2\theta$ to which $Q_\parallel$ scattering is observed [13]. The radial Patterson function $P(r)$ can be used to directly provide (i) the time-averaged radial scattering density of the membrane's molecular components as projected onto the membrane plane and rotationally-averaged about the $z$-axis perpendicular to the membrane plane and (ii) the nature of the time-averaged intermolecular order in the membrane plane in terms of the time-averaged intermolecular pair-correlation functions *if* the number of molecular components in the membrane is small (e.g. 2–3 components of dramatically different dimensions in their projection onto the membrane plane) or if the scattering amplitude of a particular molecular component can be enhanced or suppressed in an effectively isomorphous manner. In the special cases mentioned, a two-dimensional Fourier transformation of the scattering amplitude data as a function of $Q_\parallel$ can provide $\rho(x,y)$ directly [with similar spatial resolution considerations as with $P(r)$] *if* the critical phase information as a function of $Q_\parallel$ can be obtained independently [13].

The elastic scattering data along $Q_\perp$ may be analyzed via a one-dimensional Patterson function $P(z)$, which requires *only* the observable *scattering amplitude data* as a function of $Q_\perp$ (i.e., scattering-angle $2\theta$) [13, 34]. The resolution (or highest spatial frequency component) in this Patterson function derived via an appropriate one-dimensional Fourier transformation of the $Q_\perp$ scattering data depends on the largest value of $2\theta$ to which $Q_\perp$ scattering is observed. The Patterson function $P(z)$ may be utilized to directly assess the detailed nature of the order in the stacking of the membrane sheets along the stacking direction $z$ in an oriented multilayer. If the phases of the elastic scattering amplitude data along $Q_\perp$ can also be determined, an appropriate one-dimensional Fourier transformation employing *both* the *scattering amplitude* and *phase informa-*

[1] For the incident X-ray photon or neutron described by an incoming plane wave with momentum vector $\vec{k}_i$ and the scattered photon or neutron described by an outgoing spherical wave with momentum vector $\vec{k}_s$, the elastic scattering condition requires that $|\vec{k}_i| = |\vec{k}_s| \equiv 2\pi/\lambda$. The momentum transfer vector $\vec{Q}$ is defined by $\vec{Q} \equiv \vec{k}_i - \vec{k}_s$ where $|\vec{Q}| = (4\pi \sin\theta)/\lambda$ and $2\theta$ is the scattering-angle [5]. Hence, $Q_\parallel$ and $Q_\perp$ refer to elastic scattering-induced momentum transfers along the directions parallel and perpendicular to the membrane plane, respectively.

*tion* as a function of $Q_\perp$ can directly provide $\rho(z)$ for the single membrane with similar spatial resolution considerations as for the Patterson function $P(z)$ [11, 12, 24, 25, 27, 29, 34, 36]. Of the several methods currently available which are capable of providing this crucial phase information, all are based essentially on experimental access to the continuous elastic scattering along $Q_\perp$ arising from either a single membrane sheet or a special pair of membrane sheets which are stacked to form the oriented multilayer. The structural interpretation of the single-membrane scattering profile is generally not straightforward due to the nature of the projection giving rise to $\rho(z)$ which superimposes the time-averaged scattering profiles of the membrane's individual molecular components in $\rho(z)$. The only direct way to determine the time-averaged scattering profile of a particular molecular component (or submolecular fragment thereof including a single atomic site), is to significantly alter, i.e., enhance or suppress the scattering amplitude of that molecular component (or submolecular fragment thereof) relative to those of the other membrane components [6]. This alteration must be effectively isomorphous.

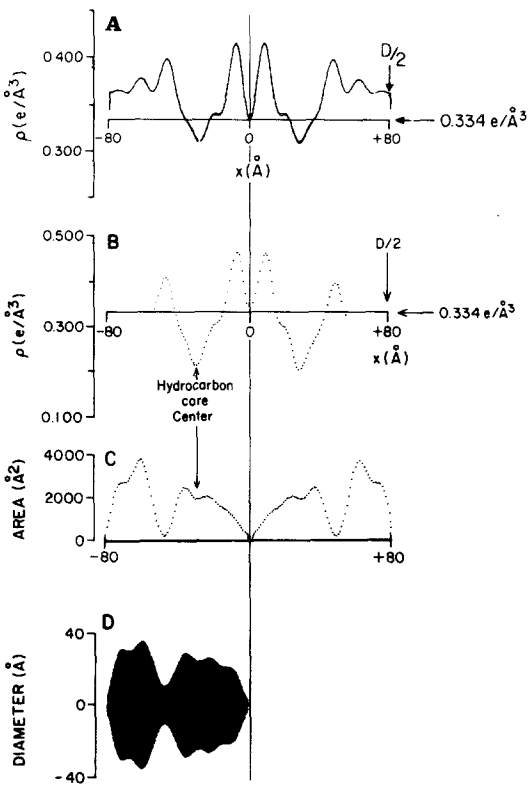


**Fig. 1.** A summary of the results of structural studies of the sarcoplasmic reticulum (SR) membrane profile at ~10 A resolution utilizing a combination of X-ray and neutron diffraction techniques as taken from reference 3 with permission of the Rockefeller University Press. *A* contains the electron density profile on an absolute scale for the unit cell of the oriented SR membrane multilayer containing the two apposed single-membrane profiles of the flattened unilamellar SR vesicle; a single-membrane profile is contained within the interval $0A \leq |x| \leq 80A$. *B* contains the separate electron density profile on an absolute scale for the asymmetric phospholipid bilayer *within* the SR membrane profile for $0A \leq |x| \leq 80A$. *C* contains the separate protein (>90% $Ca^{2+}$ ATPase) profile *within* the SR membrane profile for $0A \leq |x| \leq 80A$ expressed as the area occupied by the protein in the membrane plane as a function of the profile coordinate $x$. This *protein area profile* can also be expressed as a *protein diameter profile* (*D*) for the SR membrane protein structure cylindrically-averaged about the perpendicular to the membrane plane

## Selected Examples

At the present time, the most powerful method for enhancing the scattering amplitude of a particular molecular component (or submolecular fragment thereof) of a biological membrane in an essentially isomorphous manner, is that of neutron diffraction coupled with the perdeuteration of the molecule (or submolecular fragment thereof). The simple arithmetic *difference* between the properly *scaled* and *phased* neutron diffraction from the otherwise fully-protonated membrane containing the perdeuterated molecular component (or submolecular fragment thereof) and that from the fully protonated membrane *arises solely* from that deuterium-labeled molecular component (or submolecular component thereof). Hence, the relative position and substructure of a particular molecular component (or submolecular fragment thereof) within the profile or in-plane structure of a membrane can be directly determined utilizing the appropriate pairs of phased neutron diffraction data as a function of $Q_\perp$ or $Q_\parallel$, respectively. It might be noted that for a membrane containing $M$ molecular components, only $M$-1 components need be perdeuterated for the relative positions and substructures of all $M$ components to be determined (e.g., if the neutron-scattering profiles for the membrane itself and each of the $M$-1 components are determined, the neutron-scattering profile of the $M^{th}$ component is also determined by the difference between the membrane profile itself and the sum of the profiles of all the $M$-1 components).

We have utilized such neutron diffraction methods in conjunction with X-ray diffraction methods to determine the profile structures of the membrane's molecular components to ~10 A resolution in three different membrane systems, namely isolated sarcoplasmic reticulum membranes, reconstituted sarcoplasmic reticulum membranes, and a reconstituted photosynthetic membrane. In the case of the isolated sarcoplasmic reticulum membrane [4, 5, 16–18], the time-averaged profile structures (*see* Fig. 1) of the $Ca^{2+}$ ATPase, phospholipid

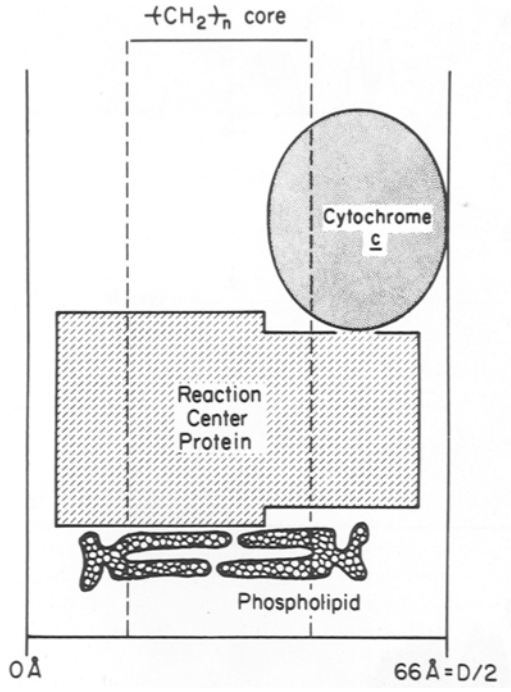


**Fig. 2.** A schematic representation of a reconstituted membrane profile consisting of cytochrome *c* bound to photosynthetic reaction centers in a phosphatidylcholine bilayer for cytochrome *c*/reaction center mole ratios $\leq 1$. The various components are drawn to scale. The reaction center protein molecule is shown as being symmetric about an axis perpendicular to the membrane plane, as the information obtained from the lamellar $Q_\perp$ diffraction data is cylindrically averaged about this axis. Cytochrome *c* is approximated as a prolate ellipsoid with dimensions of 25 × 25 × 35 $A^3$; the major axis is parallel to the membrane plane. Reproduced from reference 32 with permission of Elsevier Biomedical Press B.V.

(phosphatidylcholine and phosphatidylethanolamine) and water were determined utilizing $H_2O$/$D_2O$ exchange and the isomorphous incorporation of the biosynthetically perdeuterated phospholipids into the isolated membranes via phospholipid exchange proteins. These studies directly provided the asymmetric phospholipid bilayer profile structure and the $Ca^{2+}$ ATPase molecular structure as cylindrically-averaged about the perpendicular to the membrane plane within the overall profile structure of the isolated membrane. In the case of a reconstituted photosynthetic membrane [31, 32], the time-averaged profile structures of the photosynthetic reaction center, cytochrome *c*, phosphatidylcholine and water were determined utilizing $H_2O$/$D_2O$ exchange and the isomorphous incorporation of biosynthetically deuterated reaction centers and chemically deuterated phosphatidylcholine into the appropriately reconstituted membranes. These studies directly provided the asymmetric phospholipid bilayer profile structure, the reaction center molecular structure as cylindrically averaged about the perpendicular to the membrane plane and the profile position of the cytochrome *c* molecule electrostatically bound to the reaction center in the 1 : 1 complex within the overall profile structure of this reconstituted membrane (*see* Fig. 2).

Such neutron diffraction methods have also been used to determine the relative positions of submolecular fragments including individual atomic sites within both the profile and in-plane structures of specific membranes. In the case of the reconstituted photosynthetic membrane described above [31, 32], only the choline moiety of the phosphatidylcholine was deuterated, thereby directly providing the positions of the phospholipid headgroups and the asymmetry in the relative numbers of phospholipid molecules in the two apposed monolayers of the lipid bilayer within the profile structure of this reconstituted membrane. In the case of reconstituted sarcoplasmic reticulum membranes [19], specific atomic sites on the fatty-acid chains of the phospholipids were deuterated, thereby directly providing the different time-averaged configurations of the fatty-acid chains in the two apposed monolayers of the membrane lipid bilayer within the profile structure of this reconstituted membrane; the significant difference in the time-averaged profile structures of the two apposed phospholipid monolayers is induced by the presence of $Ca^{2+}$ ATPase protein within the membrane lipid bilayer of this reconstituted membrane. In the case of the purple membrane from *Halo bacteria* [37], specific polar and nonpolar amino acid residues of bacteriorhodopsin were deuterated biosynthetically in order to determine the positions of these residues relative to the seven $\alpha$-helices of the bacteriorhodopsin molecules in their projection onto the plane of this isolated membrane; the nonpolar residues were found to be located primarily on the surface of the seven-helix bundle in contact with the nonpolar lipid fatty-acid chain environment of the molecule within the membrane profile structure, while the polar residues were found primarily at helix-helix contacts on the interior of the seven-helix bundle.

We have also utilized equally powerful resonance X-ray diffraction methods to determine the positions of metal atoms associated with the redox centers of membrane proteins within the profile structures of reconstituted membranes [7–9, 35]. In this manner, the potential *versus* the resonance X-ray scattering from the reaction center iron atom associated with the iron-quinone primary electron acceptor complex and the iron atom associated with the heme group of the cytochrome *c* electron donor were employed to determine the positions of these two critically important metal atoms within the pro-

file structure of the reconstituted photosynthetic membrane described above with an accuracy better than ±2 A (*see* Fig. 3). It was thereby directly determined that the light-induced electron transfer reactions characteristic of the reaction center: cytochrome *c* complex produce an electric charge separation across most (approximately 2/3) of the membrane profile including virtually all of the phospholipid hydrocarbon core of this reconstituted membrane.

We might also note that the scattering amplitude of a particular molecular component in a membrane can, in principle, be altered by varying its relative concentration in the membrane of interest. However, it may be difficult to achieve a sufficient variation in an effectively isomorphous manner, i.e., without significantly perturbing the structures and/or relative positions of the membrane's components (*see* especially references [32], [19] and [20] on this point). Nevertheless, this somewhat less powerful method has been employed in several cases including the reconstituted sarcoplasmic reticulum [19] and photosynthetic membrane systems [30] described above and in the case of the gap junction [28]. In the first two cases, neutron diffraction experiments employing specifically deuterated molecular components were ultimately critical to the determination of the correct profile structures for the membrane proteins involved.

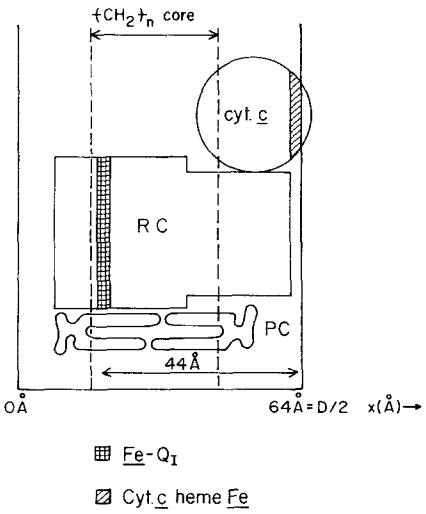


**Fig. 3.** A schematic representation to scale of our current knowledge concerning the structure of the cytochrome *c*/reaction center (*RC*) complex incorporated into the lipid (*PC*, phosphatidylcholine) bilayer of reconstituted membranes (for cytochrome *c*/reaction center mole ratios ≤1.0). The positions of the cytochrome *c* heme iron atom electron donor and the iron atom of the reaction center Fe-$Q_I$ primary quinone electron acceptor within the profile structure of the complex are indicated as determined by the resonance X-ray diffraction experiments. Reproduced from reference 7 with permission of Elsevier Biomedical Press B.V.

## Advantages/Disadvantages

The nature of the elastic scattering/diffraction techniques coupled with the generally liquid-crystalline nature of biological membrane structures necessarily limits the structural information attainable. As described in this review for the case of integral membrane proteins, generally only their time-averaged structure as cylindrically averaged about the perpendicular to the membrane plane can be derived usually to a spatial resolution of ~10 A; in special cases, the positions of certain selected atomic sites within this cylindrically averaged protein structure can be determined with a positional accuracy of ±1 A. Clearly, full three-diminsional structural information concerning the overall shape of the membrane protein (as afforded by three-dimensional image-reconstruction methods [38] applied to electron microscopic images of tilted, two-dimensionally crystalline arrays of the protein) and the detailed structure of the protein at atomic resolution (as afforded by X-ray crystallography [1] of three-dimensional crystals of the protein) will most likely be necessary to fully understand the detailed mechanism of action of these biologically important membrane proteins. However, at this time, only the elastic scattering/diffraction techniques described in this review are capable of providing substantial information concerning the intramolecular structure of a particular molecular component and its time-averaged position relative to the other molecular components of the membrane within its natural environment, namely the overall, dynamic structure of the fully-functional biological membrane itself [4, 5, 17, 30, 33].

As a result of the above considerations, *time-resolved* elastic scattering/diffraction techniques utilizing intense synchrotron and laser-plasma X-ray sources can now be employed to investigate the detailed nature of structural changes within a particular membrane component involved in the biological function of the membrane. Such time-resolved techniques have recently been utilized to describe (i) changes in the profile structure of the $Ca^{2+}$ ATPase molecule of the isolated sarcoplasmic reticulum membrane [3–5] associated with the phosphorylation of the enzyme and the "calcium occlusion" phenomenon occurring during the first 0.2–0.5 sec of the ATP-initiated calcium transport cycle at 7–8°C (*see* Fig. 4) and (ii) changes in the in-plane lattice structure of the bacteriorhodopsin molecules of the purple membrane occurring ~1 msec following

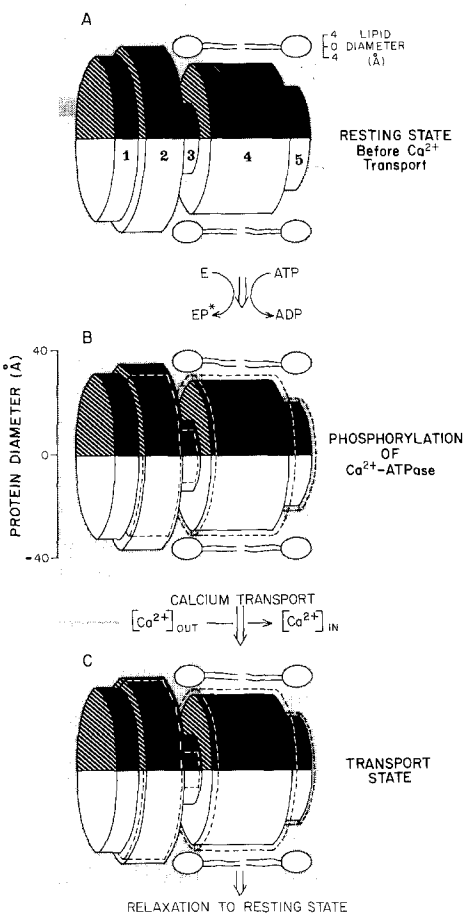


**Fig. 4.** Schematic representations of the cylindrically-averaged (about the perpendicular to the membrane plane) protein structure within the isolated sarcoplasmic reticulum membrane profile at relatively low resolution (~29 A) prior to calcium transport (*A*), in the phosphorylated intermediate state of the calcium ATPase as derived from the synchrotron radiation studies with 0.2–0.5 sec time resolution (*B*), and in the time-averaged calcium transport state as derived from the rotating-anode X-ray studies with 5.0 sec time resolution (*C*). Five cylindrical regions were used to represent the $Ca^{2+}$ ATPase at this resolution as labeled in *A*. In both *B* and *C*, the dotted-line cylinders represent the "new" state of the $Ca^{2+}$ ATPase as indicated superimposed on the "resting" state (solid line cylinders) of *A*. For both *B* and *C*, regions *2* and *3* decrease in volume, which is conservatively gained in regions *4* and *5*. Thus, the phosphorylated state and the time-averaged $Ca^{2+}$-transport state of the $Ca^{2+}$ ATPase are similar to each other and different from the resting state. Reproduced from reference 3 with permission of The Rockefeller University Press

photostimulation [14] of the bacteriorhodopsin photocycle.

## Conclusion

The elastic X-ray/neutron diffraction techniques described in this review are currently capable of providing substantial information concerning the time-averaged structures and intermolecular ordering of molecular components within a dynamic membrane structure. In addition, the time resolution of the elastic X-ray diffraction technique, afforded by intense synchrotron and laser plasma X-ray sources, now permits this structural information to be obtained over a range of time scales from nanoseconds to milliseconds and upwards following an excitation of the membrane system. This time-averaged and time-resolved structural information may provide considerable insight into structure-function relationships in biological membranes and, especially when combined with structural information on the membrane proteins involved at atomic resolution, may provide this insight at the atomic level.

## References

1. Allen, J.P., Feher, G. 1984. *Proc. Natl. Acad. Sci. USA* **81**:4795–4799
2. Bacon, G.E. 1962. *In:* Neutron Diffraction. (Chap. 2). Oxford University Press, London
3. Blasie, J.K., Herbette, L., Pascolini, D., Skita, V., Pierce, D.H., Scarpa, A. 1985. *Biophys. J. (in press)*
4. Blasie, J.K., Herbette, L., Pierce, D., Pascolini, D., Scarpa, A., Fleischer, S. 1983. *In:* International Conference on Transport ATPases. *Ann. N.Y. Acad. Sci.* **402**:478–484
5. Blasie, J.K., Herbette, L., Pierce, D., Pascolini, D., Scarpa, A., Fleischer, S., Skita, V. 1985. *In:* Structure and Function of Sarcoplasmic Reticulum. Y. Tonomura and S. Fleischer, editors. Academic, New York *(in press)*
6. Blasie, J.K., Pachence, J.M., Herbette, L. 1984. *In:* Neutrons in Biology. B.P. Schoenborn, editor. pp. 201–210. Plenum Press, New York
7. Blasie, J.K., Pachence, J.M., Tavormina, A., Dutton, P.L., Stamatoff, J., Eisenberger, P., Brown, G. 1983. *Biochim. Biophys. Acta* **723**:350–357
8. Blasie, J.K., Pachence, J., Tavormina, A., Erecinska, M., Dutton, P.L., Stamatoff, J., Eisenberger, P., Brown, G. 1982. *Biochim. Biophys. Acta* **679**:188–197
9. Blasie, J.K., Stamatoff, J. 1981. *Annu. Rev. Biophys. Bioeng.* **10**:451–458
10. Blasie, J. K., Worthington, C.R. 1969. *J. Mol. Biol.* **39**:417–439
11. Blasie, J.K., Zaccai, G., Schoenborn, B.P. 1976. *Brookhaven Symp. Biol.* **3**:58–67
12. Blaurock, A.E., King, G.I. 1977. *Science* **196**:1101–1104
13. Cowley, J.W. 1981. *In:* Diffraction Physics. North-Holland, Amsterdam
14. Frankel, R.D., Forsyth, J.M. 1985. *Biophys. J.* **47**:387–393
15. Harget, P., Krimm, S. 1971. *Acta Cryst.* **A27**:586–591
16. Herbette, L., Blasie, J.K. 1980. *In:* Calcium-Binding Proteins: Structure and Function. F.L. Siegel, E. Carafoli, R.H. Kretsinger, D.H. MacLennan, and R.H. Wasserman, editors. Elsevier/North Holland, New York
17. Herbette, L., Blasie, J.K., DeFoor, P., Fleischer, S., Bick, R.J., VanWinkle, W.B., Tate, C.A., Entman, M.L. 1984. *Arch. Biochem. Biophys.* **234**:235–242
18. Herbette, L., DeFoor, P., Fleischer, S., Pascolini, D.,

Scarpa, A., Blasie, J.K. 1985. *Biochim. Biophys. Acta (in press)*
19. Herbette, L., Scarpa, A., Blasie, J.K., Wang, C.T., Hymel, L., Seelig, J., Fleischer, S. 1983. *Biochim. Biophys. Acta* **730:**369–378
20. Herbette, L., Scarpa, A., Blasie, J.K., Wang, C.T., Saito, A., Fleischer, S. 1981. *Biophys. J.* **36:**47–72
21. Hosemann, R., Bagchi, S.N. 1962. *In:* Direct Analysis of Diffraction by Matter. North-Holland, Amsterdam
22. James, R.W. 1965. *In:* The Optical Principles of the Diffraction of X-rays. (Chapters 3 and 4) Cornell University Press, Ithaca
23. Katoaka, M., Ueki, T. 1980. *Acta Cryst.* **A36:**282–287
24. Lesslauer, W., Blasie, J.K. 1972. *Biophys. J.* **12:**175–190
25. Lesslauer, W., Cain, J., Blasie, J.K. 1972. *Proc. Natl. Acad. Sci. USA* **69:**1499–1503
26. Luckhurst, G.R., Gray, G.W. (editors) 1979. *In:* The Molecular Physics of Liquid Crystals. Academic, London
27. Makowski, L. 1981. *J. Appl. Cryst.* **14:**160–168
28. Makowski, L., Caspar, D.L.D., Phillips, W.C., Goodenough, D.A. 1977. *J. Cell Biol.* **74:**629–645
29. Moody, M.F. 1974. *Biophys. J.* **14:**697–702
30. Pachence, J.M., Dutton, P.L., Blasie, J.K. 1979. *Biochim. Biophys. Acta.* **548:**348–373
31. Pachence, J.M., Dutton, P.L., Blasie, J.K. 1981. *Biochim. Biophys. Acta* **635:**267–283
32. Pachence, J.M., Dutton, P.L., Blasie, J.K. 1983. *Biochim. Biophys. Acta* **724:**6–19
33. Pierce, D., Scarpa, A., Trentham, D.R., Topp, M.R., Blasie, J.K. 1983. *Biophys. J.* **44:**365–373
34. Schwartz, S., Cain, J.E., Dratz, E., Blasie, J.K. 1975. *Biophys. J.* **15:**1201–1233
35. Stamatoff, J., Eisenberger, P., Blasie, J.K., Pachence, J., Tavormina, A., Erecinska, M., Dutton, P.L., Brown, G. 1982. *Biochim. Biophys. Acta* **679:**177–187
36. Stroud, R.M., Agaard, D.A. 1979. *Biophys. J.* **25:**495–514
37. Trewhella, J., Gogol, E., Zaccai, G., Engelman, D.M. 1984. *In:* Neutrons in Biology. B.P. Schoenborn, editor. pp. 227–246. Plenum, New York
38. Unwin, P.N.T., Henderson, R. 1975. *J. Mol. Biol.* **94:**425–440

Received 7 November 1984